



This article was originally published in a journal published by Elsevier, and the attached copy is provided by Elsevier for the author's benefit and for the benefit of the author's institution, for non-commercial research and educational use including without limitation use in instruction at your institution, sending it to specific colleagues that you know, and providing a copy to your institution's administrator.

All other uses, reproduction and distribution, including without limitation commercial reprints, selling or licensing copies or access, or posting on open internet sites, your personal or institution's website or repository, are prohibited. For exceptions, permission may be sought for such use through Elsevier's permissions site at:

<http://www.elsevier.com/locate/permissionusematerial>

(La,Sr)(Mn,Me)O₃ manganites doped with d metals: Study of charge compensation mechanisms by crystallographic and magnetic characterizations

O.I. V'yunov^{a,*}, A.G. Belous^a, A.I. Tovstolytkin^b, O.Z. Yanchevskii^a

^a V.I. Vernadskii Institute of General & Inorganic Chemistry of UNAS, 03680 Kyiv, Ukraine

^b Institute of Magnetism of UNAS, 03142 Kyiv, Ukraine

Available online 13 March 2007

Abstract

A comparison between theoretically calculated unit cell volume and interatomic distances in the system La_{0.7}Sr_{0.3}Mn_{1-x}Me_xO_{3+δ} (where Me = Cu, Fe, Cr, Ti) and the experimental data obtained by the full-profile Rietveld X-ray analysis as well as an analysis of magnetic properties allowed us to suggest possible mechanisms of charge compensation occurring when d metals substitute for manganese. It has been shown that in the case when copper, iron, chromium and titanium ions substitute for manganese ions in the system La_{0.7}Sr_{0.3}Mn_{1-x}Me_xO₃ charge compensation is described by the model $2\text{Mn}^{3+} \rightarrow \text{Mn}^{4+} + \text{Cu}^{2+}$, $\text{Mn}^{3+} \rightarrow \text{Fe}^{3+}$, $\text{Mn}^{3+} \rightarrow \text{Cr}^{3+}$ and $\text{Mn}^{4+} \rightarrow \text{Ti}^{4+}$, respectively. In the latter case, a decrease in oxygen nonstoichiometry occurs with increasing x .

© 2007 Published by Elsevier Ltd.

Keywords: Impurities; X-ray methods; Magnetic properties; Manganites

1. Introduction

A colossal magnetoresistance is observed in lanthanum manganites with perovskite structure, that allows these materials to be considered as promising candidates for developing a new generation of magnetic sensors and magnetic information readers. Often, considerable changes in the electrical resistance of lanthanum manganites can be achieved only in strong fields or at low temperatures that dramatically restricts the range of their application in practice. Substantial modifications of the properties of manganites should be expected in the case of doping the manganese sublattice. In particular, it is possible to considerably increase the magnetoresistance of manganites by using copper dopants.¹ Iron ions considerably change magnetic, electrical and magnetoresistive properties, although do not participate in the double exchange.² Chromium ions shift the maximum of magnetoresistance to room temperature, induce the transition from antiferro- to ferromagnetic state.³ Titanium ions considerably decrease spontaneous magnetization and the Curie point.⁴ In most cases, the effect of d metals on the properties of mangan-

ites was analyzed in terms of their electronic subsystem and magnetic interactions. However, the substitution for manganese causes changes in the unit cell parameters, enhancement of structural heterogeneity, formation of vacancies in cation and anion sublattices.⁵ At present, the data concerning the effect of partial substitutions in the manganese sublattice on the magnetic properties of manganites is often incomplete and discrepant.

Therefore, the aim of this work was to investigate systematically the structure and magnetic properties of solid solutions La_{0.7}Sr_{0.3}Mn_{1-x}Me_xO_{3+δ} with quantitative calculations of unit cell volume and interatomic distances, and their comparison with experimental data in order to determine the mechanism of charge compensation occurring in the case of the substitution of manganese by d metals (Cu, Fe, Cr, Ti).

2. Experimental

Polycrystalline samples were prepared by solid-state reactions, using extra pure and reagent-grade raw materials. X-ray diffraction (XRD) measurements were performed on a DRON 4-07 powder diffractometer. Depending on chemical composition, the ceramic samples were sintered in air at the temperatures within the range of 1300–1400 °C. Structural parameters were refined by the Rietveld full-profile X-ray analysis method, using

* Corresponding author. Tel.: +380 44 4242211; fax: +380 44 4242211.
E-mail address: vyunov@ionc.kar.net (O.I. V'yunov).

the FullProf program. The Mn^{3+} and Mn^{4+} contents of the samples were determined by iodometric titration. Magnetization was measured with a Quantum Design MPMS-5S SQUID magnetometer. Ferromagnetic resonance (FMR) studies were performed on a RADIOPAN spectrometer (9.2 GHz), using samples with the dimensions $1 \text{ mm} \times 1 \text{ mm} \times 5 \text{ mm}$. The applied magnetic field was parallel to the long axis of a sample.

3. Results and discussion

After sintering ceramic $\text{La}_{0.7}\text{Sr}_{0.3}\text{Mn}_{1-x}\{\text{Cu,Fe,Cr,Ti}\}_x\text{O}_{3+\delta}$ samples had the perovskite structure with the space group $R\bar{3}c$. At $x=0$, a chemical analysis has shown oxygen nonstoichiometry to be $\delta_0=0.035$, and the fraction of Mn^{4+} in the total manganese amount to be 0.38. The experimental parameters of the crystal structure of ceramic samples were compared with the calculated values on the assumption of different charge compensation mechanisms (Table 1). NMR spectra have shown that manganese in the manganites is in both Mn^{3+} and Mn^{4+} states.⁶ Mn^{2+} can appear only when there are a considerable number of vacancies in the lanthanum sublattice.⁵ Therefore, in the present work, we assumed that manganese is in the oxidation states +3 and +4 only. For the calculation we used the interrelation between the free volume of the unit cell, V_f , with the tolerance factor t of $\text{A}_{1-a}\text{A}'_a\text{B}_{1-b}\text{B}'_b\text{O}_{3\pm\delta}$ perovskite, deduced in Ref.⁷: $V_f = (V_{\text{meas}} - V_{\text{occ}})/V_{\text{meas}} = (1.20 \pm 0.09) - (0.95 \pm 0.09)t$, where V_{occ} is the occupied unit cell volume, which is equal to the sum of the volumes of both ions and vacancies calculated using ionic radii.⁸ The radii of vacancies were determined using formulas presented in Ref.⁷ Occupied unit volume

and radius of vacancies, which are interrelated, have been determined by method of successive approximations. Also, we took into account the coexistence of both high-spin (HS) and low-spin (LS) states of Mn^{3+} ions, whose ratio in the solid solution $\text{La}_{0.8}\text{Sr}_{0.2}\text{MnO}_3$ was determined at room temperature as $\text{Mn}_{\text{HS}}^{3+}:\text{Mn}_{\text{LS}}^{3+} \approx 3:1$.⁹

Fig. 1a shows that the experimental values of the unit cell volume and interatomic distances in the $\text{La}_{0.7}\text{Sr}_{0.3}\text{Mn}_{1-x}\text{Cu}_x\text{O}_{3+\delta}$ as a function of x value are in good agreement with the calculated data according the model X ($2\text{Mn}^{3+} \rightarrow \text{Mn}^{4+} + \text{Cu}^{2+}$). The character of M_s versus x dependence for the $\text{La}_{0.7}\text{Sr}_{0.3}\text{Mn}_{1-x}\text{Cu}_x\text{O}_{3\pm\delta}$ system considerably changes near $x=0.07$ (Fig. 2): for low x (≤ 0.07) the saturation magnetization is almost constant and agrees with the calculated dependence for $2\text{Mn}^{3+} \rightarrow \text{Mn}^{4+} + \text{Cu}^{2+}$ model (X), whereas at $x > 0.07$ it significantly decreases with increasing x . In the calculations, we assumed that the magnetization of $\text{Mn}_{\text{HS}}^{3+}$ (spin $S=2$) is $4 \mu_B$; $\text{Mn}_{\text{LS}}^{3+}$ ($S=1$) = $2 \mu_B$; Mn^{4+} ($S=3/2$) = $3 \mu_B$.¹⁰ For the samples with $x \leq 0.07$, the FMR spectrum is a single line, but for the sample with $x > 0.07$, two well-defined absorption lines are observed, which correspond to two different magnetic phases (Fig. 3). These data are in good agreement with the determined limits of the existence of homogeneous ferromagnetic phase for the model X (see Table 1).

A characteristic feature of the $\text{La}_{0.7}\text{Sr}_{0.3}\text{Mn}_{1-x}\text{Fe}_x\text{O}_3$ system is that Fe^{3+} ions like Mn^{3+} ions can be in both high-spin and low-spin state. Experimental dependences for the unit cell parameters were successfully described only for $\text{Mn}^{3+} \rightarrow \text{Fe}^{3+}$ model (IX) on the assumption that the ratio between ions in high-spin and low-spin state for iron is the same as for manganese:

Table 1
Models of charge exchange in $\text{La}_{0.7}\text{Sr}_{0.3}\text{Mn}_{1-x}\text{Me}_x\text{O}_{3+\delta}$ system (Me = Cu, Fe, Cr, Ti)

Model	Me				Model of cation vacancies ($\delta > 0$)	Model of anion vacancies ($\delta < 0$)	x_c	x_{\min}	x_{\max}
	Cu	Fe	Cr	Ti					
I			+		$\text{Mn}^{3+} \rightarrow \text{Me}^{6+} + 1/2(\text{V}_A + \text{V}_B)$			0.24	
II			+		$\text{Mn}^{4+} \rightarrow \text{Me}^{6+} + 1/3(\text{V}_A + \text{V}_B)$			0.24	
III			+		$\text{Mn}^{3+} \rightarrow \text{Me}^{5+} + 1/3(\text{V}_A + \text{V}_B)$			0.24	
IV			+		$2\text{Mn}^{4+} \rightarrow 2\text{Me}^{5+} + 1/3(\text{V}_A + \text{V}_B)$			0.24	
V			+	+	$2\text{Mn}^{3+} \rightarrow 2\text{Me}^{4+} + 1/3(\text{V}_A + \text{V}_B)$			0.24	
VI			+		$3\text{Mn}^{4+} \rightarrow 2\text{Mn}^{3+} + \text{Me}^{6+}$			0.07	
VII			+		$2\text{Mn}^{4+} \rightarrow \text{Mn}^{3+} + \text{Me}^{5+}$			0.11	
VIII		+	+	+	$\text{Mn}^{4+} \rightarrow \text{Me}^{4+}$			0.24	
IX	+	+	+	+	$\text{Mn}^{3+} \rightarrow \text{Me}^{3+}$				0.24
X	+	+	+		$2\text{Mn}^{3+} \rightarrow \text{Mn}^{4+} + \text{Me}^{2+}$				0.08
XI	+				$3\text{Mn}^{3+} \rightarrow 2\text{Mn}^{4+} + \text{Me}^{1+}$				0.048
XII	+	+	+	+	$2\text{Mn}^{4+} \rightarrow 2\text{Me}^{3+} - 1/3(\text{V}_A + \text{V}_B)$	$2\text{Mn}^{4+} \rightarrow 2\text{Me}^{3+} + \text{V}_O^{2-}$	0.070	0.24	
XIII	+	+	+		$2\text{Mn}^{3+} \rightarrow 2\text{Me}^{2+} - 1/3(\text{V}_A + \text{V}_B)$	$2\text{Mn}^{3+} \rightarrow 2\text{Me}^{2+} + \text{V}_O^{2-}$	0.070		0.24
XIV	+				$\text{Mn}^{3+} \rightarrow \text{Me}^{1+} - 1/3(\text{V}_A + \text{V}_B)$	$\text{Mn}^{3+} \rightarrow \text{Me}^{1+} + \text{V}_O^{2-}$	0.035		0.24
XV	+	+	+		$\text{Mn}^{4+} \rightarrow \text{Me}^{2+} - 1/3(\text{V}_A + \text{V}_B)$	$\text{Mn}^{4+} \rightarrow \text{Me}^{2+} + \text{V}_O^{2-}$	0.035	0.24	
XVI	+				$2\text{Mn}^{4+} \rightarrow 2\text{Me}^{1+} - (\text{V}_A + \text{V}_B)$	$2\text{Mn}^{4+} \rightarrow 2\text{Me}^{1+} + 3 \text{V}_O^{2-}$	0.024	0.24	
XVII	+	+	+	+	$3/2\text{O}_2 \rightarrow \text{ABO}_3 + (\text{V}_A + \text{V}_B) + 6\text{h}^+$				

Notes: (1) In the models I–V, δ increases with Me content, in the models VI–XI it does not change, and in the models XII–XVI, it decreases down to zero at x_c . In the model XVII, only intrinsic Schottky defects are considered; the introduced dopant is not involved explicitly in the model.¹³ (2) The sign “+” denotes the models under analysis, and color denotes the models determined in substituted manganites by structure analysis and magnetic measurements. (3) In the calculations, we assumed that the ratio $\text{Mn}_{\text{HS}}^{3+}:\text{Mn}_{\text{LS}}^{3+}$ is retained in substituted manganites. (4) x_{\min} and x_{\max} correspond to the concentration limits of nonmagnetic manganese-substituting dopants within which a homogeneous ferromagnetic phase exists (these values are derived from the conditions $C_{\text{Mn}}^{4+} = 0.18$ and 0.50, respectively).¹⁵

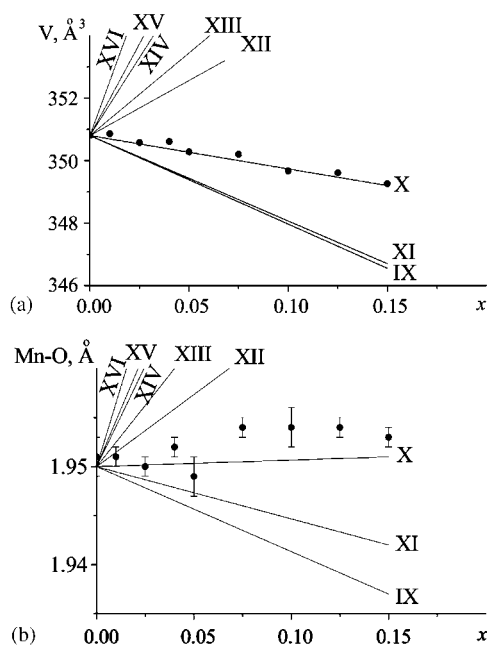


Fig. 1. Unit cell volume V (a) and interatomic Mn–O distance (b) vs. copper content for $\text{La}_{0.7}\text{Sr}_{0.3}\text{Mn}_{1-x}\text{Cu}_x\text{O}_{3\pm\delta}$: experimental plot is presented in comparison with the calculated results. The numbers on the curves denote the models listed in Table 1.

$\text{Mn}_{\text{HS}}^{3+}:\text{Mn}_{\text{LS}}^{3+} \sim 3:1$ (Fig. 1b). With increasing iron content the shape of FMR spectra does not change considerably over a wide concentration range,¹¹ which corresponds to the dopant concentration limits for the model X (see Table 1).

The experimental dependence of the unit cell volume and interatomic distances in the $\text{La}_{0.7}\text{Sr}_{0.3}\text{Mn}_{1-x}\text{Cr}_x\text{O}_3$ system is in good agreement with two dependences calculated according to the following charge compensation models: $\text{Mn}^{3+} \rightarrow \text{Cr}^{3+}$ (IX) and $2\text{Mn}^{3+} \rightarrow \text{Mn}^{4+} + \text{Cr}^{2+}$ (X). Within the range of chromium concentrations ($0 \leq x \leq 0.12$) the shape of FMR spectrum is practically unchanged. It corresponds to the model (IX)

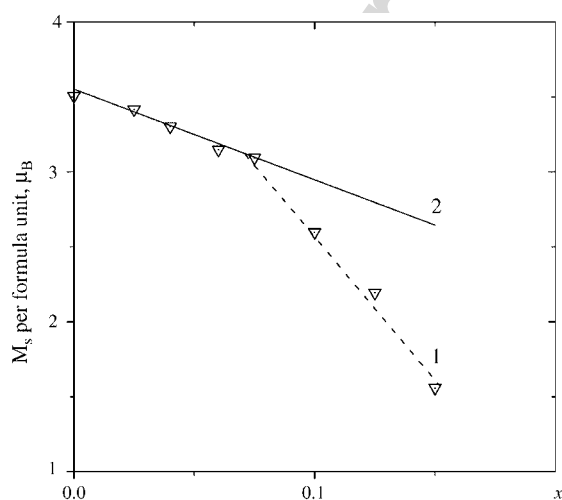


Fig. 2. Measured (1) and calculated (2) saturation magnetization for $\text{La}_{0.7}\text{Sr}_{0.3}\text{Mn}_{1-x}\text{Cu}_x\text{O}_{3\pm\delta}$ at liquid helium temperature in the magnetic field of 4000 kA/m.

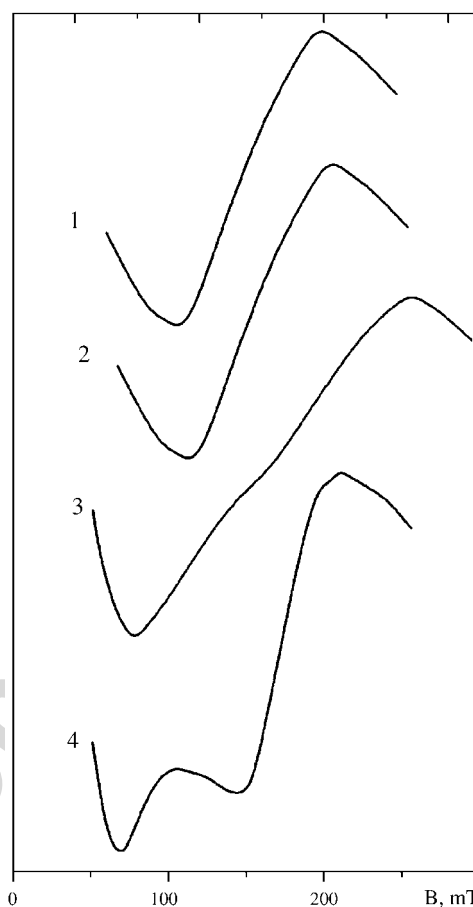


Fig. 3. FMR spectra of $\text{La}_{0.7}\text{Sr}_{0.3}\text{Mn}_{1-x}\text{Cu}_x\text{O}_{3\pm\delta}$ with $x=0$ (1); 0.025 (2); 0.05 (3); 0.08 (4) liquid nitrogen temperature.

$\text{Mn}^{3+} \rightarrow \text{Cr}^{3+}$, for which the range of homogeneous ferromagnetic phase is considerably wider as compared to that of the model (X) $2\text{Mn}^{3+} \rightarrow \text{Mn}^{4+} + \text{Cr}^{2+}$. However, if chromium participates in the double exchange, then taking into account the identical configuration of the outer electronic shells for Mn^{4+} and Cr^{3+} ($3d^3$) and for Mn^{3+} and Cr^{2+} ($3d^4$), this would result in the $3d^4 \rightarrow 3d^3$ model (IX), for which the homogeneous ferromagnetic phase exists in a wide range of substitutions in the manganese sublattice. Therefore, the results of magnetic studies do not allow a correct distinguishing between the models (IX) and (X) for the case when chromium partly substitutes for manganese.

The experimental dependence of the unit cell volume for $\text{La}_{0.7}\text{Sr}_{0.3}\text{Mn}_{1-x}\text{Ti}_x\text{O}_{3\pm\delta}$ on the titanium content is nonlinear (Fig. 4) and cannot be described in terms of the simple models, including the $\text{Mn}^{4+} \rightarrow \text{Ti}^{4+}$ (VIII) model assumed in Ref.⁴ At the same time, for $x > 0.17$, the $V(x)$ dependence seems to be in agreement with the calculations performed for $\delta=0$ within the above model. Therefore, we can conclude that at $x > 0.17$ the model $\text{Mn}^{4+} \rightarrow \text{Ti}^{4+}$ exists, whereas in the range of $0 \leq x \leq 0.17$ an additional model should be suggested, which involves a decrease in the oxygen nonstoichiometry δ with increasing x . The δ value may decrease as a result of the processes XII or XVII (see Table 1). However, the process XII corresponds to a different model of charge compensation and, therefore, to a dif-

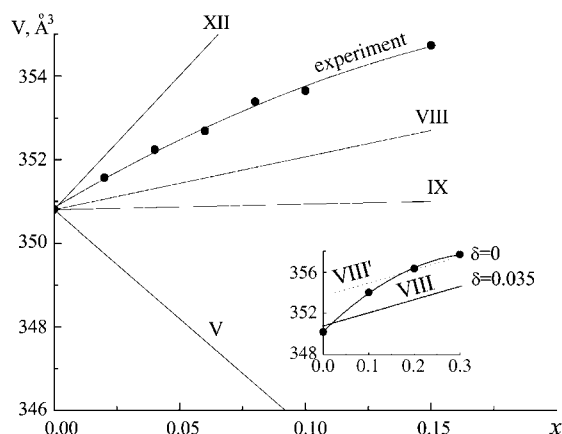


Fig. 4. Unit cell volumes of $\text{La}_{0.7}\text{Sr}_{0.3}\text{Mn}_{1-x}\text{Ti}_x\text{O}_{3\pm\delta}$ obtained from experimental data (points; the inset shows the data from Ref. [4]) and calculated (lines). The numbers on the curves denote the models listed in Table 1.

ferent $V(x)$ dependence at $x_C = 0.07$, which is not supported by the experimental data (see Fig. 4). When titanium substitutes for manganese in the $\text{La}_{0.7}\text{Sr}_{0.3}\text{Mn}_{1-x}\text{Ti}_x\text{O}_{3\pm\delta}$ system in the range $0 \leq x \leq 0.17$, the number of intrinsic defects changes like that in the $\text{La}_{1-x}\text{Sr}_x\text{MnO}_{3\pm\delta}$ system when strontium substitutes for lanthanum.¹² This process is described by the model XVII, in which Schottky defects are involved.¹³ This model leads to small variations in the magnetic properties with titanium content up to $x < 0.17$.¹⁴

4. Conclusions

According to the results of a comprehensive analysis of the concentration dependences of unit cell volume, interatomic Mn–O distances, saturation magnetization, and ferromagnetic resonance spectra of $\text{La}_{0.7}\text{Sr}_{0.3}\text{Mn}_{1-x}\text{Me}_x\text{O}_3$ system (where $\text{Me} = \text{Cu}, \text{Fe}, \text{Cr}, \text{Ti}$), we have demonstrated that when copper substitutes for manganese the charge compensation is in accordance with the $2\text{Mn}^{3+} \rightarrow \text{Mn}^{4+} + \text{Cu}^{2+}$ model. When iron substitutes for manganese the charge compensation can be represented by the model $\text{Mn}^{3+} \rightarrow \text{Fe}^{3+}$. At the same time, when chromium substitutes for manganese the charge compensation can be represented by the model $\text{Mn}^{3+} \rightarrow \text{Cr}^{3+}$, but the model $2\text{Mn}^{3+} \rightarrow \text{Mn}^{4+} + \text{Cr}^{2+}$ is also possible if chromium ions take

part in the double exchange. It has been shown that when titanium substitutes for manganese the charge compensation occurs via the $\text{Mn}^{4+} \rightarrow \text{Ti}^{4+}$ model with a simultaneous decrease in the oxygen nonstoichiometry δ with increasing x .

References

1. Nguyen, C., Niem, P. Q., Nhat, H. N., Luong, N. H. and Tho, N. D., Influence of Cu substitution for Mn on the structure, magnetic, magnetocaloric and magnetoresistance properties of $\text{La}_{0.7}\text{Sr}_{0.3}\text{MnO}_3$ perovskites. *Physica B*, 2003, **327**, 214–217.
2. Li, Y.-D., Zhang, J.-H., Xiong, C.-S. and Liao, H.-W., Ferromagnetism and magnetoresistance in $\text{La}_{0.67}\text{Sr}_{0.33}\text{Fe}_{0.07}\text{Mn}_{0.93}\text{O}_3$. *J. Am. Ceram. Soc.*, 2000, **83**, 980–982.
3. Kallel, N., Dhahri, J., Zemni, S. et al., Effect of Cr-doping in $\text{La}_{0.7}\text{Sr}_{0.3}\text{Mn}_{1-x}\text{Cr}_x\text{O}_3$ $0 \leq x \leq 0.5$. *Phys. Status Solidi*, 2001, **184**, 319–325.
4. Kallel, N., Dezanneau, G., Dhahn, J., Oumezzine, M. and Vincent, H., Structure, magnetic and electrical behaviour of $\text{La}_{0.7}\text{Sr}_{0.3}\text{Mn}_{1-x}\text{Ti}_x\text{O}_3$ with $0 \leq x \leq 0.3$. *J. Magn. Mater.*, 2003, **261**, 56–65.
5. Dagotto, E., Motta, T. and Moreo, A., Colossal magnetoresistant materials: the key role of phase separation. *Phys. Rep.*, 2001, **344**, 1–153.
6. Abou-Ras, D., Boujelben, W., Cheikh-Rouhou, A., Pierre, J., Renard, J.-P., Reversat, L. et al., Effect of strontium deficiency on the transport and magnetic properties of $\text{Pr}_{0.7}\text{Sr}_{0.3}\text{MnO}_3$. *J. Magn. Magn. Mater.*, 2001, **233**, 147–154.
7. Ullmann, H. and Trofimenko, N., Estimation of effective ionic radii in highly defective perovskite-type oxides from experimental data. *J. Alloys Compd.*, 2001, **316**, 153–158.
8. Shannon, R. D., Revised effective ionic radii and systematic studies of interatomic distances in halides and chalcogenides. *Acta Cryst.*, 1976, **A32**, 751–767.
9. Kamata, H., Yonemura, Y., Mizusaki, J., Tagawa, H., Naraya, K. and Sasamoto, T., High temperature electrical properties of the perovskite-type oxide $\text{La}_{1-x}\text{Sr}_x\text{MnO}_{3-\delta}$. *J. Phys. Chem. Solids*, 1995, **56**, 943–950.
10. Haghir-Gosnet, A.-M. and Renard, J.-P., CMR manganites: physics, thin films and device. *J. Phys. D: Appl. Phys.*, 2003, **36**, R127–R150.
11. Yanchevskii, O. Z., V'yunov, O. I., Belous, A. G. and Tovstolytkin, A. I., Crystallographic electrical, and magnetic properties of the system $\text{La}_{0.7}\text{Sr}_{0.3}\text{Mn}_{1-x}\text{Fe}_x\text{O}_3$. *Low Temp. Phys.*, 2006, **32**, 134–138.
12. Mizusaki, J., Mori, N., Takai, H., Yonemura, Y., Minamiue, H., Tagawa, H. et al., Oxygen nonstoichiometry and defect equilibrium in the perovskite-type $\text{La}_{1-x}\text{Sr}_x\text{MnO}_{3\pm\delta}$. *Solid State Ionics*, 2000, **129**, 163–177.
13. Nowotny, J. and Rekas, M., Defect chemistry of $(\text{La}, \text{Sr})\text{MnO}_3$. *J. Am. Ceram. Soc.*, 1998, **81**, 67–80.
14. Yanchevskij, O. Z., V'yunov, O. I., Belous, A. G., Tovstolytkin, A. I. and Kravchik, V. P., Synthesis and characterization of $\text{La}_{0.7}\text{Sr}_{0.3}\text{Mn}_{1-x}\text{Ti}_x\text{O}_3$ manganites. *Phys. Solid State*, 2006, **48**, 709–716.
15. Akimoto, T., Maruyama, Y., Moritomo, Y. and Nakamura, A., Antiferromagnetic metallic state in doped manganites. *Phys. Rev.*, 1998, **B57**, 5594–5597.